The Behaviour of Water-Mists in Hot Air Induced by a Room Fire: Effect of the Initial Size of Droplets

fire

MDPI

Article

The Behaviour of Water-Mists in Hot Air Induced by a Room Fire: Effect of the Initial Size of Droplets

H. M. Iqbal Mahmud [1,2,*], Graham Thorpe [2] and Khalid A. M. Moinuddin [2]

[1] Department of Civil Engineering, Khulna University of Engineering & Technology, Khulna 9203, Bangladesh
[2] Institute for Sustainable Industries and Liveable Cities, Victoria University, P.O. Box 14428, Melbourne, VIC 8001, Australia
* Correspondence: iqbal.mahmud@ce.kuet.ac.bd

Abstract: This paper presents work on investigating the effect of the initial size of water mist droplets on the evaporation and removal of heat from the fire-induced hot gas layer while travelling through the air in a compartment. The histories of the temperature, diameter and position of droplets with different initial diameters (varied from 100 µm to 1000 µm) are determined considering surrounding air temperatures of 75 °C and 150 °C and a room height of 3.0 m. A water droplet evaporation model (WDEM) developed in a previous study (Fire and Materials 2016; 40:190–205) is employed to navigate this work. The study reveals that tiny droplets (for example, 100 µm) have disappeared within a very short time due to evaporation and travelled a very small distance from the spray nozzle because of their tiny size. In contrast, droplets with a larger diameter (for example, 1000 µm) reached the floor with much less evaporation. In the case of this study, the relative tiny droplets (≤200 µm) have absorbed the highest amount of energy from their surroundings due to their complete evaporation, whereas the larger droplets have extracted less energy due to their smaller area/volume ratios, and their traverse times are shorter. One of the key findings of this study is that the smaller droplets of spray effectively cool the environment due to their rapid evaporation and extraction of heat from the surroundings, and the larger droplets are effective in traversing the hot air or smoke layer and reaching the floor of the compartment in a fire environment. The findings of this study might help in understanding the behaviour of water-mist droplets with different initial diameters in designing a water-mist nozzle.

Keywords: water-mist; droplet size; evaporation; equilibrium temperature; fire; hot air

Citation: Mahmud, H.M.I.; Thorpe, G.; Moinuddin, K.A.M. The Behaviour of Water-Mists in Hot Air Induced by a Room Fire: Effect of the Initial Size of Droplets. *Fire* **2022**, *5*, 116. https://doi.org/10.3390/fire5040116

Academic Editors: Song Lu, Changcheng Liu, Guohui Li and Paweł Wolny

Received: 5 June 2022
Accepted: 10 August 2022
Published: 15 August 2022

1. Introduction

Water in the form of a mist has been shown to be an effective fire extinguishing agent. The water-mist fire suppression system (WMFSS) uses smaller size of water droplets compared to the conventional water sprinkler droplets and suppresses the fire by the displacement of oxygen by means of evaporation of water droplets [1,2]. The National Fire Protection Association (NFPA) defined water mist as a water spray in which 99% of the water is in droplets whose diameter (D_{v99}) is less than 1000 µm [3]. During the past several years, water mist technology has been developed and regarded as a promising substitute since it can extinguish fires quickly with little water and, at the same time, without damaging the environment [4,5]. In the analysis of the suppression mechanism of fire by water droplets, it is imperative to understand the evaporation behaviour of a single droplet travelling through a fire-induced smoke layer and the phenomena connected with the evaporation process.

The literature is replete with studies on the heating and evaporation of water from single droplets suspended in high-temperature environments [6–10]. Strizhak et al. [8] conducted a series of experiments to investigate the heating and evaporation of suspended water droplets with diameters varying from 1.8 to 3 mm in a hot air flow with temperatures

up to 800 °C. Volkov and Strizhak [7] performed experiments on water droplets suspended in the air with the size ranging from 1 to 2 mm at high air temperature varying from 100 to 800 °C, and measured the evaporation rate and profile of droplet size, and recorded the time of their existence. Sobac et al. [9] developed a quasi-steady model to analyse the evaporation process of a suspended water droplet in air. Thielens et al. [10] developed a two-zone model for heating an evaporating water droplet suspended and exposed to hot airflow. They used the model to predict the lifetime and saturation temperatures of droplets.

However, it is worthy to note that in these studies, the droplets were suspended in a stationary position; hence, the effect of momentum transfer of the droplets was not of primary importance. A defining feature of water-mist nozzles is that they produce fine mists consisting of tiny droplets with diameters of less than 1000 µm. The fine mists exhibit fog-like behaviour that renders their fire suppression mechanism quite different from conventional water sprays that comprise larger droplets [11]. Studies of the interaction of traditional sprinkler spray with hot air or smoke layers [12–19] have focused mainly on the convective heat transfer phenomena between the large water droplets and the layer of hot air. It was found that the evaporation of larger droplets discharged from conventional sprinklers had not been affected significantly by the fire plume [12–17]. It has also been confirmed from the previous study that large size of water droplets produced by sprinklers can remove only between 11% and 26% of the heat produced by fire [19–21].

Water-mist droplets can cool the surrounding air and attenuate thermal radiation, and the water vapour produced by evaporation reduces the fuel vapour/air ratio by displacing oxygen [22–27]. Evidence supports the idea that water-mist spray can remove 100% of the heat produced by a fire either by extinguishing it or allowing enough evaporation to keep the compartment's temperature at or below the boiling point of water [21,28]. However, not all droplets evaporate before striking burning surfaces, and this provides a direct method of suppressing fires [23,24,29,30]. In particular, the initial diameter of the droplets and the surrounding environment are the main factors determining whether a droplet can travel through the hot smoke layer or evaporate entirely before reaching the floor. However, it is imperative to understand the evaporative behaviour of a single water mist droplet travelling through the hot air in a fire-induced room environment based on heat and mass transfer fundamentals in the droplet.

Therefore, the objective of this paper is to investigate the evaporation behaviour of a single droplet while travelling through a fire-induced smoke layer in a room. The profiles of the temperature, diameter and position of the droplet are studied with different initial drop sizes under two different room environments. In addition, the suspension time in the air and the evaporation rate of the droplets are explored. A previously developed water droplet evaporation model (WDEM) by the same authors [11] is used to facilitate this investigation.

Several important parameters should be considered while analysing the behaviour of a single droplet travelling through the hot smoke layer. The tiny droplets of water that comprise fine mists have a higher surface area/volume ratio. This results in their rapid evaporation, and their movement is highly responsive to their local environment [11]. As a result, water droplets emanating from a nozzle, the diameter and velocity change continuously due to evaporation, and this affects the drag coefficient. Furthermore, the Reynolds number (Re) affects the heat and mass transfer coefficient between water and air. The relative humidity (RH) of the surrounding air significantly affects the evaporation of droplets. Lower humidity contributes to a higher evaporation rate of the water droplet. In a fire scenario, when sprinkler systems are activated at a temperature of 60 °C, say, the relative humidity (RH) of the surrounding air is very low, typically 5%. It is worth noting that some of these effects were not considered in the many previous studies, for example, the studies in the reference [31–34]. However, the above-mentioned phenomena should be considered in the movement of water droplets in hot air induced by a room fire.

The novelty of the model used in this study is that the following parameters are considered: (i) the contribution of radiation emanating from the flame and the surrounding boundary walls to the rate of evaporation of water droplets, (ii) the change of Re and drag coefficient of the droplets with time and position, (iii) the effect of high mass transfer rate due to the high evaporation of droplets resulting from a high air temperature and low relative humidity, (iv) the change of droplet momentum, due to the change of droplet velocity and diameter and (v) the variable thermo-physical properties of water and air. The law of conservation of mass, momentum and energy was used to evaluate the heat and mass transfer phenomena in an air-droplet system in connection with the effect of change of momentum of an evaporating droplet.

2. Description of the Model

The evaporation processes experienced by a moving droplet encompass simultaneous heat, mass, and momentum transfer between the particle and surrounding air. Momentum transfer affects the motion of the particle, mass transfer results in changes in the size of the particle, and heat transfer determines the temperature of the particle. Interestingly, these mechanisms are inextricably related [31]. The model developed by these authors accounts for the effect of a mass transfer rate due to high temperature and low humidity. The accuracy of the predictions of temperature, velocity, diameter, evaporation rate and other parameters related to the behaviour of droplets is enhanced by considering the changes in the diffusivity of the air-water system, density and latent heat of vaporisation of water with the change of temperature.

In this model, the shape of droplet is assumed to be spherical as this would not give any significant error in the computation [35]. The droplet is considered as a 'lumped mass' as the Biot number is very low [36]; as a result, the temperature distribution in the droplet was assumed to be uniform during the evaporation. This considerably simplified the analysis of the overall computational process, since it avoided the need for a conjugate heat-conduction analysis for the internal transient temperature-distribution inside the droplet [34]. The air velocity in the hot air layer is supposed to be insignificant as the droplet is supposed to travel through hot air layer, which is not nearby the fire source. The heat transfer from the ambient air to the droplet is due to forced convection.

In this study, the collision and coalescence of droplets are considered to be negligible. This assumption is reasonable for a low volume of water spray that results in dilute droplet loading in the air [37–39]. In fact, the water mist spray nozzle is designed to use a small amount of water. As a result, the mass concentration of water in the air in terms of droplet number per cubic meter of air is comparatively low. This causes a higher value of the ratio of droplet–droplet separation distance to droplet diameter. Under this condition, the probability of droplet coalescence is negligible [37]. This phenomenon was also addressed by Ananth and Mowrey [38], and Sikanen et al. [40].

The smoke layer or hot air is assumed to be in quasi steady-state, and this attribute to a stable smoke layer which is formed finally when the ceiling jet reaches the boundary wall and rebounded several times [32]. This assumption is more appropriate for the nozzles and smoke layers, which are located away from the fire source or burning object [11]. This is also supported by the experimental observations in articles of [18,41].

The details of the mathematical models of mass and heat transfer and momentum of a droplet are summarized in the following sub-sections and are also available in details in the previously published paper [11].

According to the theory of mass transfer, mass flux per unit area from the interfacial surface of a water droplet is proportional to the mass concentration difference across the boundary layer of the droplet [42]. Therefore, the rate of change of droplet diameter with time can be determined from the following equation:

$$\frac{dD}{dt} = 2h_m \frac{(\rho_s - \rho_\infty)}{\rho_w} \quad (1)$$

In the above equation, h_m is the mass transfer coefficient, ρ_w is the density of water, and ρ_s and ρ_∞ are the mass concentration of water vapour on the droplet surface and in the air, respectively. The mass concentration of water particle at the surface of the droplet depends on the partial pressure of vapour at the droplet surface. In thermodynamic equilibrium state, the partial pressure of the vapour at the droplet surface depends on the surface temperature [32]. Under this condition, evaporation keeps the droplet surface in a saturated condition until the droplet is totally vaporized due to heat and mass transfer [43]. The vapour concentration at the surface is the saturated mass fraction of air at temperature of droplet. As the mass concentration of water particle depends on vapour pressure of water, this can be found from the ideal gas equation of state [11].

The mass transfer coefficient, h_m, can be calculated by using the correlation for Sherwood number, Sh, where Sh is $h_m D/\mathrm{D}_{AB}$ [44] and D_{AB} is the mass diffusivity coefficient in a binary system of A and B; here, binary system is air and water. The correlation of Sherwood number can be expressed as [45],

$$Sh = 2.0 + 0.216\left(Re^{\frac{1}{2}}\ Sc^{\frac{1}{3}}\right)^2,\ For\ \left(Re^{\frac{1}{2}}\ Sc^{\frac{1}{3}}\right) < 1.4 \tag{2}$$

$$Sh = 1.56 + 0.616\left(Re^{\frac{1}{2}}\ Sc^{\frac{1}{3}}\right),\ For\ \left(Re^{\frac{1}{2}}\ Sc^{\frac{1}{3}}\right) \geq 1.4 \tag{3}$$

In the above equations, the Schmidt number, Sc, is a dimensionless number defined as the ratio of momentum diffusivity (viscosity) and mass diffusivity, and is used to characterize fluid flows in which there are simultaneous momentum and mass diffusion convection processes.

When a droplet is exposed to a higher temperature, it receives heat from the surrounding and temperature increases to a threshold limit, at a given pressure, and this is known as steady state or equilibrium temperature. At this temperature, the water droplet changes its phase from liquid to vapour, keeping the droplet surface in steady state condition of temperature until the droplet is entirely vaporised [46]. Under this condition, the heat of vaporisation is supplied to the droplet surface from surrounding air, flame and hot objects. Therefore, according to the law of conservation of energy, the net convective and radiative heat transfer to the droplet surface is equal to the heat accumulated in the droplet plus heat leaving the droplet due to evaporation of water particles from the surface of the droplet. Considering the rate of change of temperature and mass, the transient equation of the conservation of heat can be expressed as:

$$\begin{aligned} c_{pw} m \tfrac{dT}{dt} = {} & h_c A(T_\infty - T) \\ & + [\sigma \varepsilon F A\left\{\left(T_f + 273.15\right)^4 - (T + 273.15)^4\right\} \\ & + \sigma \varepsilon A(1 - F)\left\{(T_{bw} + 273.15)^4 - (T + 273.15)^4\right\}] - \tfrac{dm}{dt} L \end{aligned} \tag{4}$$

Here, c_{pw} is the specific heat capacity of water, h_c is the convective heat transfer coefficient, and L is the latent heat of vaporisation of water. In the above equation, the first part on the right side of the equation is due to convective heat transfer from air to droplet, the second and third parts are due to radiative heat transfer from fire flame and boundary wall to the droplet, respectively, and the fourth part contributes to the evaporation of water droplets.

The convective heat transfer coefficient, h_c, can be calculated by using the correlation for the Nusselt number, Nu, where Nu is $h_c \mathrm{D}/k_a$ [44]. The correlation for the Nusselt number can be expressed as [45],

$$Nu = 2.0 + 0.216\left(Re^{\frac{1}{2}}\ Pr^{\frac{1}{3}}\right)^2,\ For\ \left(Re^{\frac{1}{2}}\ Pr^{\frac{1}{3}}\right) < 1.4 \tag{5}$$

$$Nu = 1.56 + 0.616\left(Re^{\frac{1}{2}}\ Pr^{\frac{1}{3}}\right),\ For\ \left(Re^{\frac{1}{2}}\ Pr^{\frac{1}{3}}\right) \geq 1.4 \tag{6}$$

These relationships were found to be in good agreement with the numerical and experimental results [47]. In those above equations, Pr is Prandtl number which is the ratio of viscous diffusion rate (v) to thermal diffusion rate (α) of air, i.e., $Pr = \frac{v}{\alpha} = \frac{c_p \mu}{k}$ and Re is Reynolds number, which is the ratio of inertia force to viscous force, i.e., $Re = \frac{\rho v D}{\mu}$.

The velocity of the droplet can be obtained by solving the equation of conservation of momentum. When a body is falling from a height, body force (or weight) works in the downward direction and resistance of air drag and buoyancy force work in the upward direction. The equation of momentum for a water droplet, traveling in air, can be obtained by Newton's second law of motion. Therefore, the momentum equation for a water droplet with mass m, diameter D and relative velocity v, can be written as:

$$\frac{d(mv)}{dt} = mg - \frac{1}{2}\rho_a v^2 C_d A_{proj} - \frac{1}{6}\rho_a \pi D^3 g \tag{7}$$

In the above equation, ρ_a is the density of air, C_d is the coefficient of drag, g is the acceleration due to gravity, A_{proj} is the projected area of the droplet and v is the velocity of the droplet. The term in the left side of the equation is the rate of change of momentum of the droplet; The first term on the right side is the force acting on the droplet due to gravity, the second term is the drag, sometimes called air resistance or fluid resistance, refers to forces which act on the droplet in the opposite direction of the movement, and the third term is the buoyancy force work in the upward direction. In case of the movement of water droplet, mass, m, and velocity of droplet, v, both of them are changing with time. Therefore, simplifying the above equation, the rate of change of velocity of the droplet can be expressed as:

$$\frac{dv}{dt} = g\frac{(\rho_w - \rho_a)}{\rho_w} - \frac{3}{4}\frac{C_d \rho_a v^2}{\rho_w D} - \frac{3v}{D}\frac{dD}{dt} \tag{8}$$

It is to be noted that C_d for a droplet depends on Re, which is based on the air-droplet relative velocity. Brown and Lawler [48] proposed a correlation between drag coefficient and Re, and compared it with 178 experimental data points. The proposed correlation was found to be quite satisfactory in relation to the experimental data in the range of $0 \leq Re < 2 \times 10^5$. The correlation by Brown and Lawler [48] is used here for the calculation of C_d. It is:

$$C_d = \frac{24}{Re}\left(1 + 0.15\, Re^{0.681}\right) + \frac{0.407}{1 + \frac{8710}{Re}} \tag{9}$$

The velocity of a droplet is given by:

$$\frac{dy}{dt} = v \tag{10}$$

in which y is the vertical distance from where the mist is dropping down. Overall, Equations (1), (4), (8) and (10) are solved simultaneously to obtain D, T, v and y, respectively, of the droplet with respect to time. A Lagrangian approach is used to track the movement of water droplets, as this is well suited to tracking the dispersed particle flow.

The use of coefficients, h_m and h_c are limited to the case of low-mass-transfer-rate. In case of high temperature and low humidity, the evaporation rate is high and this invokes the high mass transfer rate and affects the heat transfer rate, as well. Therefore, corrections are also applied to calculate the mass and heat transfer coefficient to account for the effect of high mass and heat mass rate in the evaporation of droplets. The density of humid air, saturation vapour pressure, latent heat of vaporisation of water and other thermos-physical properties of air, such as viscosity, thermal conductivity and specific heat capacity of air were accounted in the model. The details of the correction factors, thermos-physical properties or vapour and air, and computational procedures of the model are presented in reference [11].

3. Validation of the Model

The developed model (WDEM) was validated and verified against experimental data by Gunn and Kinzer [49] and theoretical data of adiabatic saturation temperature, respectively. The results of this model were also compared with that of a computational fluid dynamics (CFD)-based fire model, fire dynamics simulator (FDS) [50]. The prediction of the developed model agreed well with the calculated values by FDS. The model (WDEM) was also compared with two other models by Li and Chow [32] and Barrow and Pope [34]. The details of the validation and verification of the model are available in the previous version of the paper as in reference [11].

In this section, the proposed model is further validated using the data of CARAIDAS experiments [51]. The details of the experimental set-up and results are also presented in the publication by Plumecocq et al. [52]. The conditions of the experiments used in the CARAIDAS are mentioned in Table 1.

Table 1. Test conditions of three EVAP tests of the CARAIDAS program [52] used as benchmarks in this work.

Test Condition	Air Conditions			Spray Droplets at Injection (z = 0 m)		
	P (Pa)	T (°C)	RH (%)	T (°C)	D (μm)	v (m/s)
EVAP4	10^5	47	12	25	387	1.44
EVPA8	10^5	106	<1	25	414	1.55
EVPA11	10^5	147	<1	28	423	1.59

These three experiments were performed at atmospheric pressure and low relative humidity which are usually corresponding to gas conditions that could be met in the fire room prior the activation of a spray system [52]. These conditions of the experiments are incorporated in the evaporation model (WDEM) to evaluate the droplet diameters. The predictions of the model are compared with the experimental data and the results are presented in Table 2.

Table 2. Comparison between the evaporation model predictions and CARAIDAS test results [52] for the evolution of droplets diameter.

Test Condition	D (μm) at z = 2.51 m			D (μm) at z = 4.39 m		
	Test	WDEM	Diff	Test	WDEM	Diff
EVAP4	375	375	0%	363	366	1%
EVPA8	393	382	−3%	363	356	−2%
EVPA11	393	377	−4%	342	335	−2%

The results show that the predicted data is very close to the experimental measurements. The difference between predicted data and experimental results is not more than 4%, which validating the model on the CARAIDAS experiments. In the following section, the developed model (WDEM) is used to investigate the parameters relating to the behaviour of a droplet travelling through two different hot air environments with variable initial droplet sizes.

4. Results and Discussion

Evaluation of the effect of initial sizes of droplets is conducted in this study at high air temperature in the vicinity of fire in a room. The initial air condition of the room, i.e., temperature and relative humidity, is taken to be 20 °C and 50%, respectively, and the initial temperature of the water drops is taken to be 20 °C. However, smoke will be produced in the room due to a fire, and the room temperature will be raised. Here two temperature conditions are considered for the analysis.

(i) Condition 1: the smoke layer temperature is raised to 75 °C, at which temperature the water-mist nozzle is activated. This activation temperature is typical of commercial water mist and sprinkler systems [53]; Due to the high temperature, the relative humidity of the air falls to 3%.

(ii) Condition 2: the smoke layer temperature is raised to 150 °C. The temperature of a smoke layer produced by fire usually varies between 100 and 180 °C and can reach up to 200 °C [54–57] based on the distance from the fire source. Therefore, an average value of 150 °C is considered for the analysis. When the air temperature is beyond 100 °C, there is no longer any limit to the amount of water vapour that can be stored in the air [32].

The potential travel path of the droplets is taken to be the height of a room in a residential or commercial building, i.e., 3.0 m. The elapsed time begins when the water droplets emanate from a ceiling-mounted nozzle and terminate when they strike the floor. The airflow is assumed to be in a quiescent state, as the droplets are considered to be located away from the fire. In the experimental study, it can also be observed that the hot air layer is almost steady when the nozzle is located away from the fire source [18,41]. A schematic of the computational domain of droplet movement is presented in Figure 1.

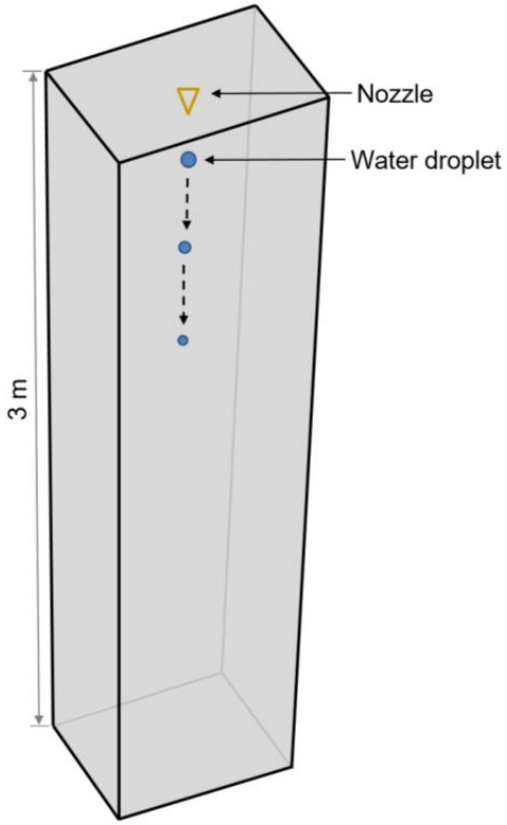

Figure 1. Schematic of the computational domain for the movement of droplet.

A sensitivity analysis has been conducted before performing the analysis using the computational model. The governing differential equations are discretised and solved explicitly using a forward differencing technique temporally. The initial conditions of a droplet, i.e., initial diameter (D), temperature (T), velocity (v) and position (y), as well as the relevant thermo-physical boundary conditions of water and air, are specified. The discretisation of the equation depends on the change of parameters with time steps (Δt).

Therefore, the histories of D, T, v, and y should be independent of the time step, Δt. In this study, it has been found that if the ratio of droplet diameter to time step is less than or equal to 0.01, the solution is independent of the time step. A time-step independence test for a droplet with a diameter of 200 μm was performed as an example. The temperature

(T) of a droplet with three different time steps of 0.1, 0.01 and 0.001 s are computed and compared. Numerical instabilities are observed when the time step is 0.1 s. However, for time steps of 0.01 and 0.001 s, the temperature and velocity measurements are similar and consistent. As a result, a calculating time step of 0.01 s can be used. A graphical presentation of the results is shown in Figure 2.

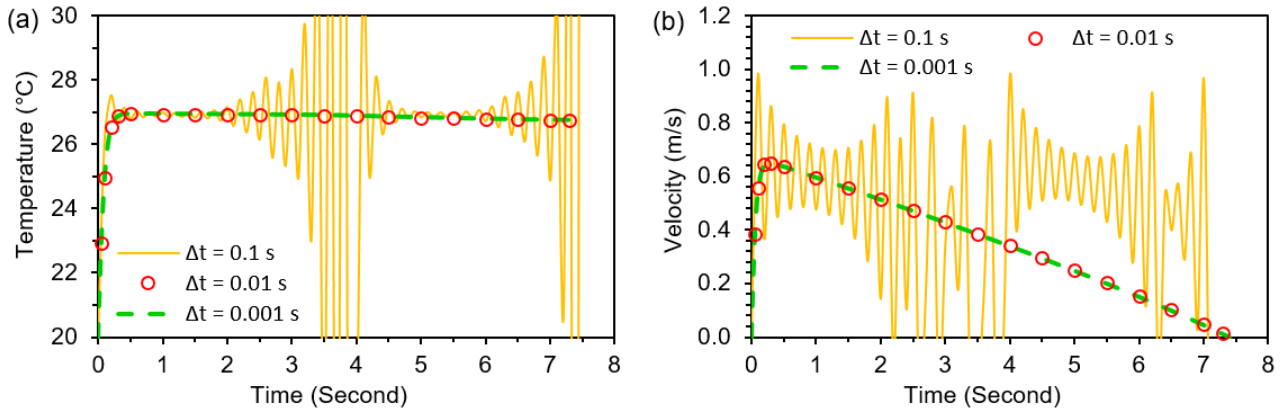

Figure 2. Sensitivity analysis of the computational model; (**a**) temperature (T), and (**b**) velocity (v).

Once the time step is selected, the parametric study is conducted using the model and the results are presented in the following sub-sections. The temperature histories of droplets for two different temperature conditions are calculated with initial diameters of 100, 200, 300, 400, 500, 750 and 1000 µm, and the results are illustrated in Figure 3. It is found that the temperature of the droplets has increased until they have reached an equilibrium temperature at which the heat gained by convection for the air is equal to that of the heat loss by the evaporation of water. The temperature at this condition is known as equilibrium temperature or steady-state temperature.

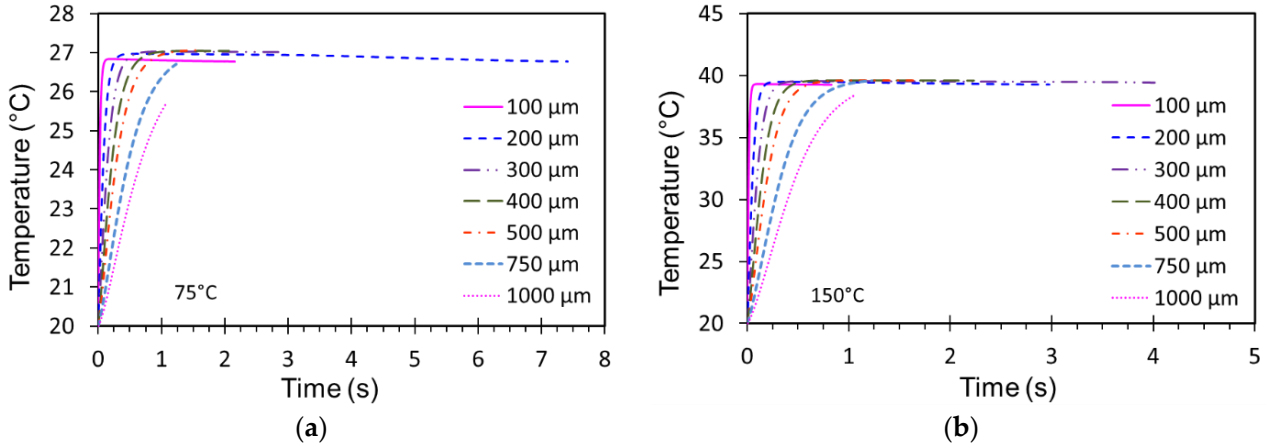

Figure 3. The effect of the initial size of diameter on the temperature trajectories of droplets; (**a**) condition 1 (75 °C); and (**b**) condition 2 (150 °C).

From the analysis, it has also been found that the smaller the initial diameter of the droplets, the less time it has taken to reach the equilibrium thermal condition. Concomitantly, as the size of the droplets has increased, the time to reach the equilibrium thermal condition has become higher. However, the equilibrium temperature has only a weak dependence on the size of the droplets, and it depends principally on the temperature and relative humidity of the air. For the condition of 75 °C air temperature, 20 °C water temperature and 3% relative humidity, the equilibrium temperature of droplets is about 27 °C, and for the second condition of 150 °C air temperature, 20 °C water temperature and 0.5% relative humidity, the equilibrium temperature is about 39 °C. It is important to

note that the smaller size of droplets have reached to the equilibrium temperature earlier compared to the bigger droplets. Furthermore, the droplets have reached the thermal equilibrium state earlier at condition 2.

The diameter and position history of the droplet with different initial sizes are analysed for condition 1, and the results are presented in Figure 4. Two factors influence the longevity of the droplets in the air of a room, namely the rate at which they evaporate, and the time it takes to reach the floor. For example, it can be seen from Figure 4 that droplet with an initial diameter of 100 µm has been evaporated completely within 2.16 s, but fall a mere 0.25 m from the nozzle. On the other hand, the droplet with an initial diameter of 200 µm has had a relatively longer existence of 7.42 s in the air; and because of this, they have travelled 2.6 m distance from the nozzle. However, the droplets with an initial diameter of 300 µm or more scarcely change their diameters before impacting the floor. Furthermore, the higher the diameter above 300 µm, the shorter the suspension time in the air.

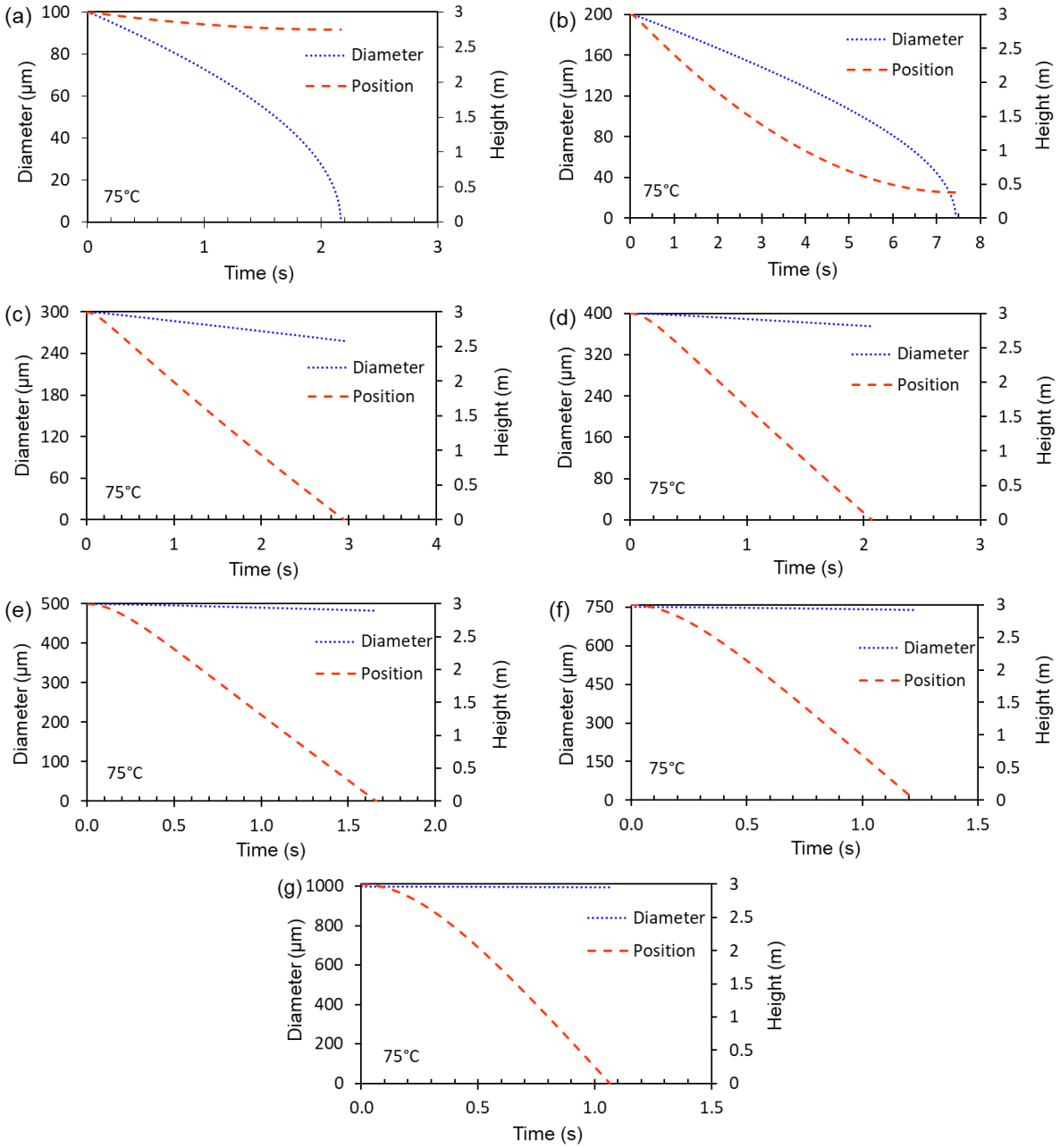

Figure 4. Diameter and position history of droplets with different initial diameters at condition 1 (75 °C); (**a**) 100 µm; (**b**) 200 µm; (**c**) 300 µm; (**d**) 400 µm; (**e**) 500 µm; (**f**) 750 µm; and (**g**) 1000 µm.

This is because the smaller droplet has higher value of surface area to volume ratio compared to the larger droplet and as a result, it enhances the rate of evaporation of the droplets by extracting heat from the hot gases and smoke layer [13,58]. The finer the droplets the greater the surface area to volume ratio of water. For example, the surface area to volume ratio of a 300 μm droplet is 20, whereas it is 30 and 60 for 200 μm and 100 μm diameter of droplet, respectively. Furthermore, the smaller droplet reaches to equilibrium temperature earlier compared to the larger droplet (as seen in Figure 3). As a result, the evaporation of water particles from the droplet surface also starts earlier in the smaller droplet. Furthermore, as the smaller droplet has lower momentum, it is suspended in the air for a longer time, if it has not completely disappeared due to evaporation. This also leads to a higher suspension time for the smaller droplet and results in a decrease in the diameter of the droplet due to evaporation.

Similar phenomena are also observed for condition 2, as shown in Figure 5. The droplets of diameter 100 and 200 μm are evaporated completely before they have reached the floor. In particular, the 100 μm droplet disappears within 1 s after leaving the nozzle. Thus, the droplet has travelled only about 0.1 m in the room. In contrast, the 200 μm droplet is sustained in the air for about 3 s and travelled about 1 m. Compared to condition 1, these two sizes of droplets have taken a lower time to evaporate as intuitively expected. They have also travelled a shorter distance due to faster evaporation at higher temperatures. The evaporation of 300 μm droplet is also significant. The diameter of this droplet has been reduced by half due to evaporation. The suspension time of this droplet is about 4 s which is the highest lifetime compared to the other size of droplets. However, the droplets with an initial diameter of 400 μm or more scarcely change their diameters before impacting the floor in both conditions. Furthermore, the travel time of the droplets with the initial diameter of 400 to 1000 μm is almost the same for both conditions.

It can be seen from Figures 4 and 5 that the higher the diameter above 300 μm, the shorter the suspension time in the air. Therefore, from the point of view of fire extinguishment, it appears that the smaller size of droplets (in this case, 100 and 200 μm) may be effective in cooling the air within an enclosure but they are less likely to penetrate a layer of hot air and extinguish conflagrating surfaces on the floor of an enclosure. On the other hand, the larger the diameter, the higher the possibility of penetrating a layer of hot air and reaching the floor, however, the larger droplet does not absorb heat from the surrounding. Actually, water mists (containing tiny droplets) and water sprays (containing large droplets) have quite different *modi operandi*. The fine particles with diameters that constitute water mists not only attenuate thermal radiation [59] but also reduce their environment's temperature due to their high surface area per unit volume and their high rate of vaporisation. In contrast, the larger droplets that comprise water sprays are likely to penetrate fires and cool surfaces of the undergoing combustion.

The velocity and corresponding vertical positions of droplets with different initial sizes in a room for condition 1 are illustrated in Figure 6. It is observed that the droplets with initial diameters of 100 and 200 μm initially accelerate in the gravitational field but decelerate quite markedly as their diameters decrease due to evaporation. These two smaller diameters of droplets reach their thermal equilibrium states after 0.081 and 0.284 s, respectively, and they continue to evaporate until they disappear. As the diameter of 100 and 200 μm droplets reduces due to evaporation, their velocity also reduces with time. However, the change in velocity of droplets with diameters greater than 400 μm is insignificant because there is little change in their diameters, as found in Figure 4.

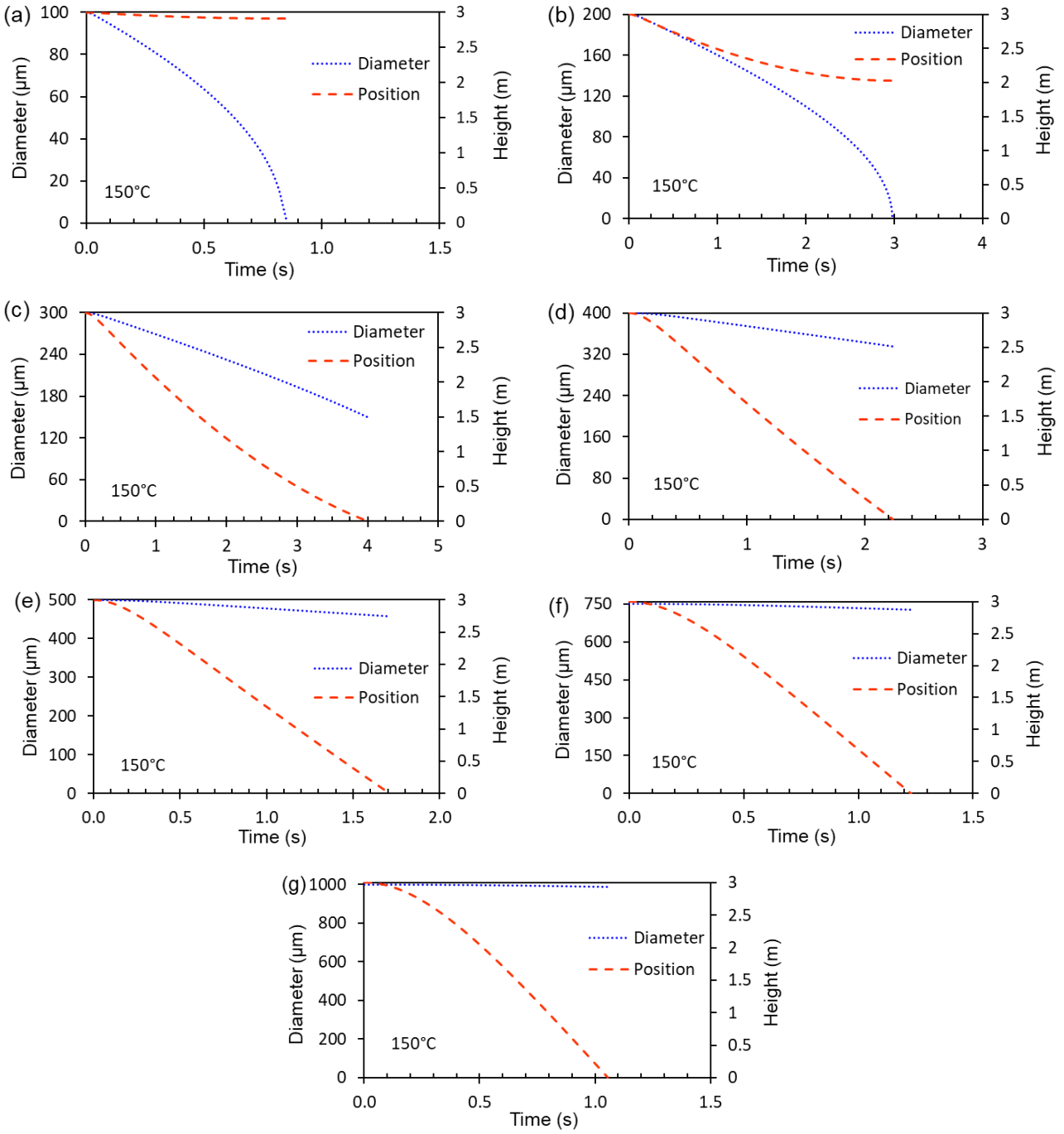

Figure 5. Diameter and position history of droplets with different initial diameters at condition 2 (150 °C); (**a**) 100 μm; (**b**) 200 μm; (**c**) 300 μm; (**d**) 400 μm; (**e**) 500 μm; (**f**) 750 μm; and (**g**) 1000 μm.

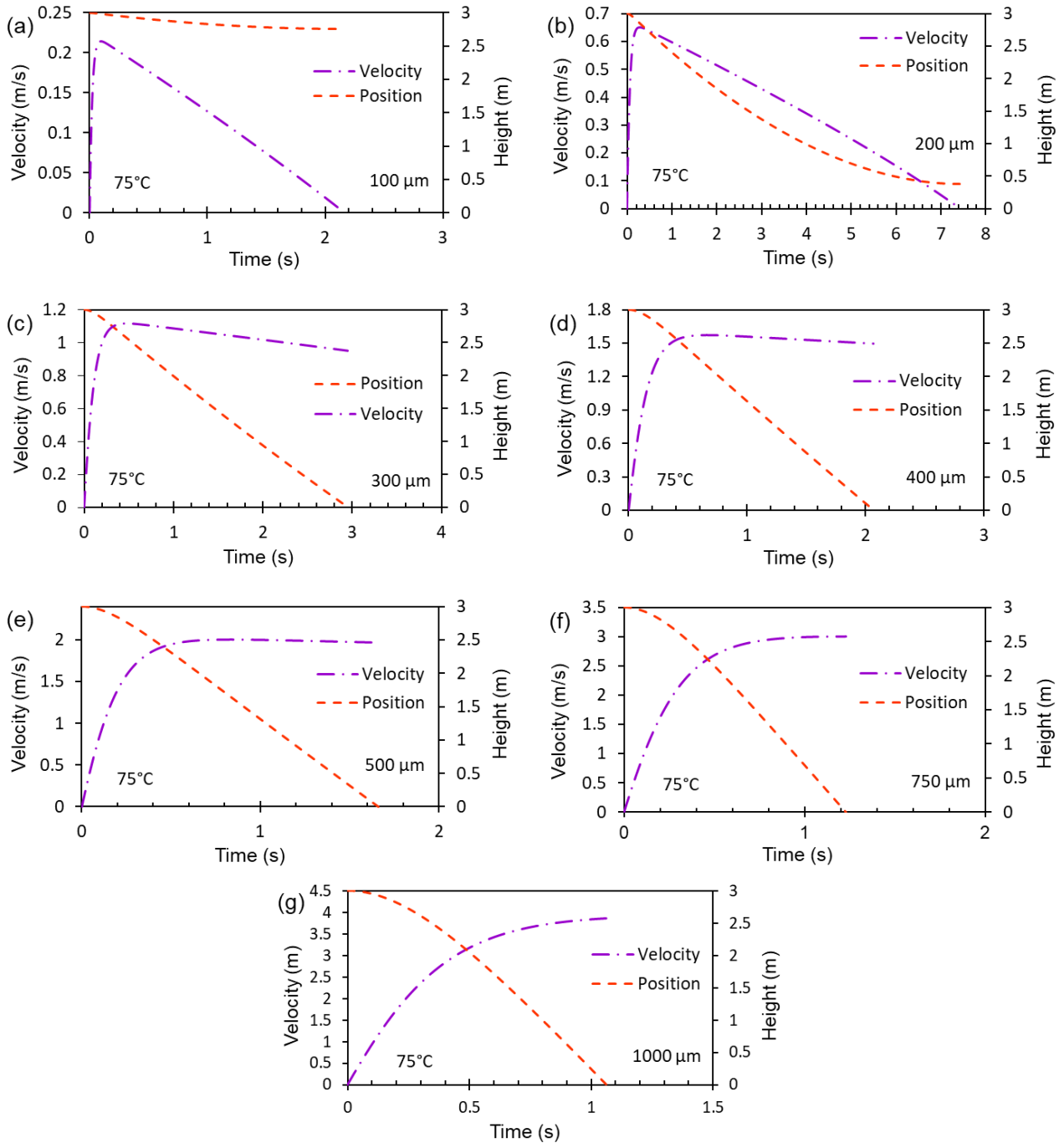

Figure 6. Velocity and position history of droplets with different initial drop sizes for condition 1 (75 °C); (**a**) 100 µm; (**b**) 200 µm; (**c**) 300 µm; (**d**) 400 µm; (**e**) 500 µm; (**f**) 750 µm; and (**g**) 1000 µm.

The velocity and position histories of droplets with different initial sizes for temperature condition 2 are demonstrated in Figure 7. The velocity of 100 µm droplets decreases quickly due to the reduction in the diameter of droplets caused by the rapid evaporation at high temperature. The velocity of the droplet of 200 µm is also reduced to zero, and the droplet is sustained in the air for 3 s. However, the droplet of 400 µm and larger have higher speeds due to their larger size. Similarly to condition 1, the change in velocity of droplets with diameters greater than 400 µm is negligible because there is little change in their diameters.

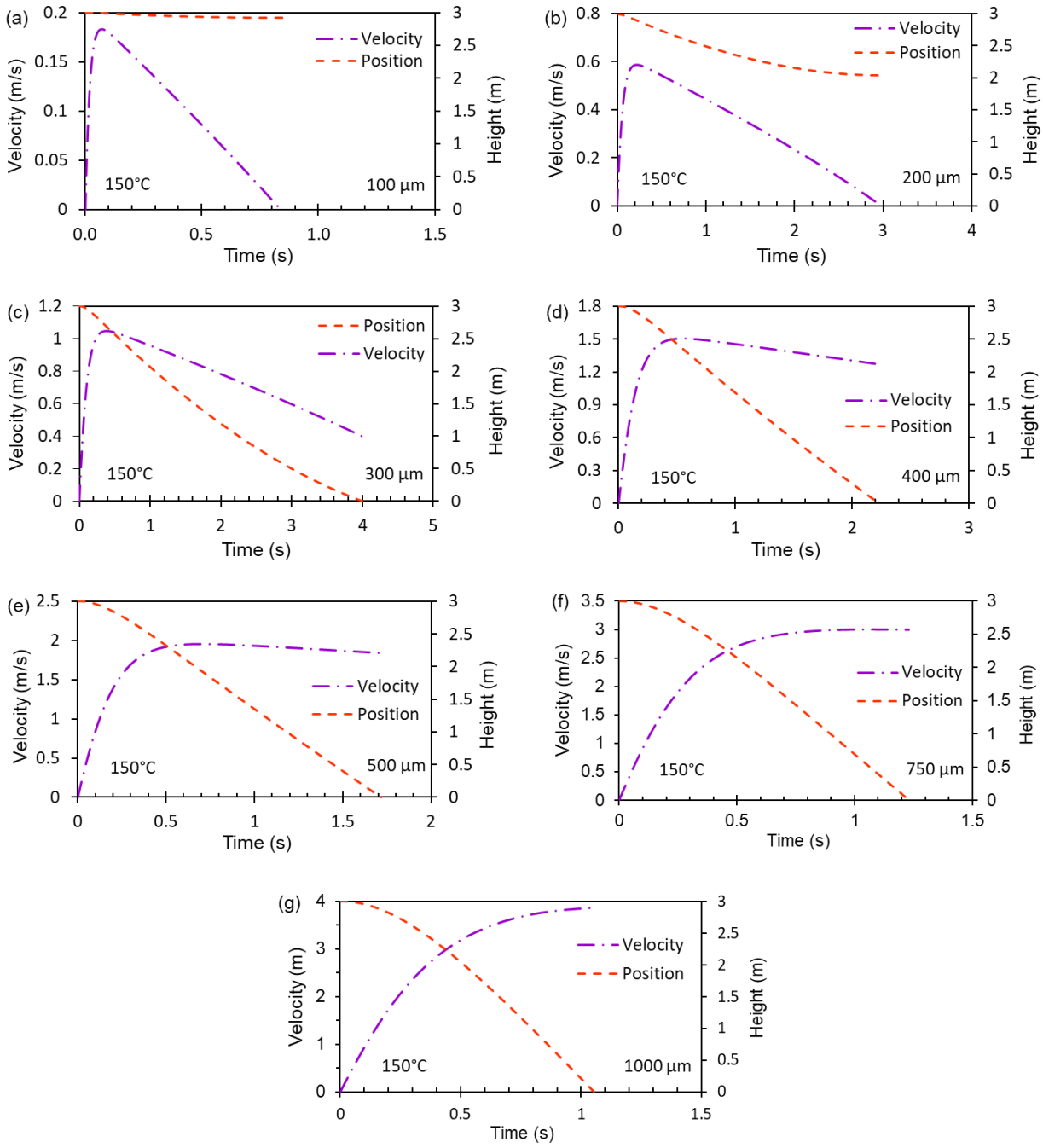

Figure 7. Velocity and position history of droplets with different initial drop sizes for condition 2 (150 °C); (**a**) 100 µm; (**b**) 200 µm; (**c**) 300 µm; (**d**) 400 µm; (**e**) 500 µm; (**f**) 750 µm; and (**g**) 1000 µm.

Interestingly, the analysis shows that, in condition 1, the 200 µm droplet has the highest lifetime compared to the other size of droplets; whereas in condition 2, the 300 µm droplet has the highest life time of the droplets. This is because, due to higher temperature in condition 2, the 200 µm droplet has taken less time to evaporate compared to condition 1. However, the 300 µm droplet does not evaporate significantly in condition 1, whereas it does in condition 2 as the air temperature is higher. As a result, due to the reduction in diameter of the 300 µm droplet in condition 2, the momentum of the droplet also reduces. This results in longer suspension time of the 300 µm droplet in the air in condition 2. Therefore, if the boundary condition of environment (smoke temperature, relative humidity, room height) changes, the suspension time of droplets also will be different.

The net heat flux rates in the droplets for condition 1 and 2 are presented in Figure 8. This heat flux is the resultant of the convective and radiative heat transfer to the droplet and the heat leaving the droplet due to evaporation of water particle from the droplet. The initial peak of the heat flux rate is due to the rise in temperature by the convection and radiation without significant evaporation of water particle from the droplet. When the droplet has attained the equilibrium temperature, the resultant is lowered due to leaving of heat by the evaporation of water particle from the droplet. The results show that the larger the droplet sizes, the higher the initial peak and also the higher the air temperature, the greater the net heat flux rate.

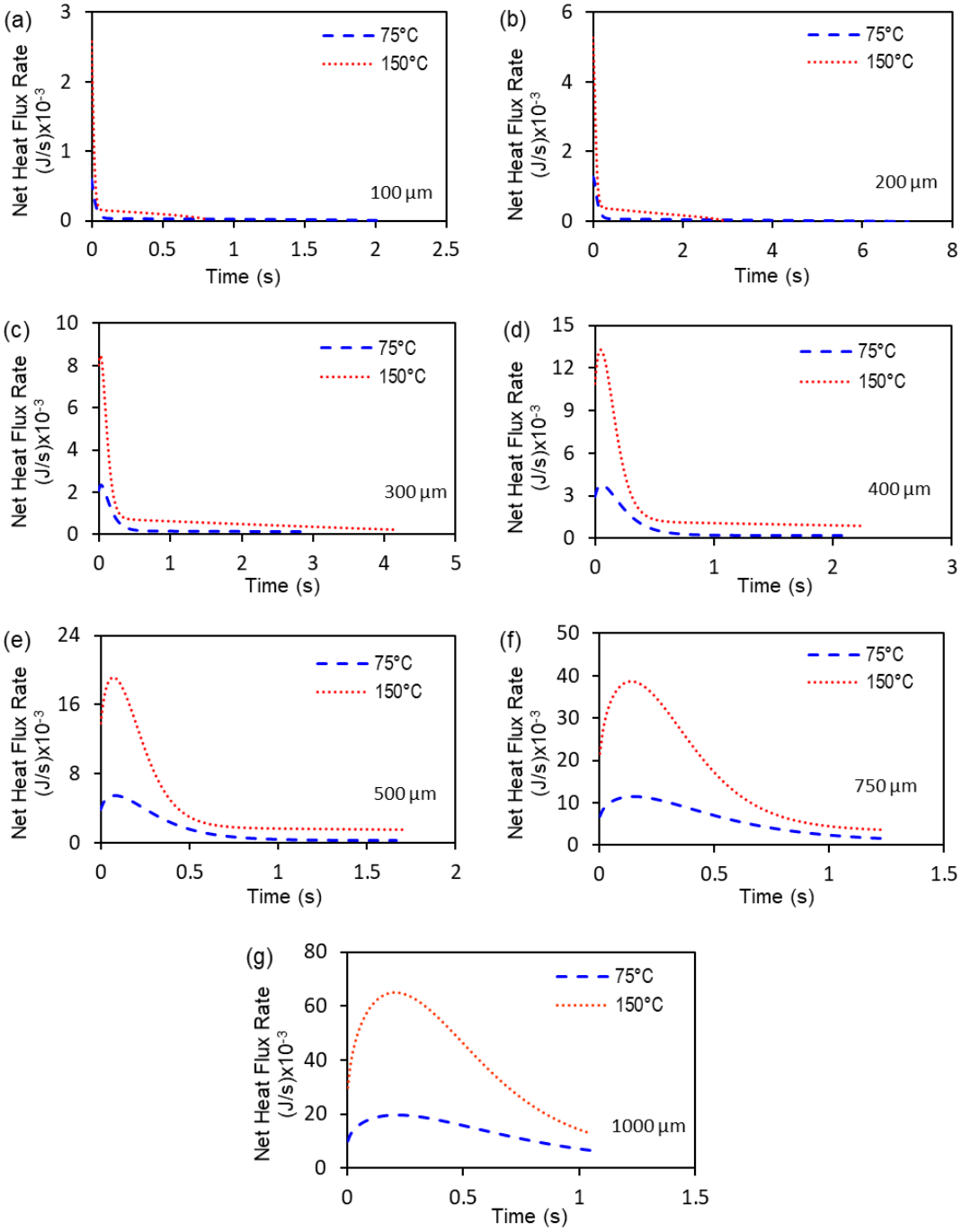

Figure 8. The net heat flux rate in the droplets for condition 1 and 2; (**a**) 100 µm; (**b**) 200 µm; (**c**) 300 µm; (**d**) 400 µm; (**e**) 500 µm; (**f**) 750 µm; and (**g**) 1000 µm.

The heat and mass transfer coefficients of the droplets for condition 1 and 2 are presented in Figure 9. The smaller size of the droplet has exhibited a higher heat and mass transfer rate. This is because smaller size of the droplet has reached equilibrium temperature earlier and started to evaporate significantly compared to the larger size of droplet; eventually, this causes higher heat and mass transfer rate for the smaller size of droplets. Specifically, in case of the 100 and 200 µm droplets a sudden rise in the heat and mass transfer coefficient is observed. This happens when the droplets have become very tiny due to evaporation; as a result, this has caused rapid evaporation to the tiny droplets.

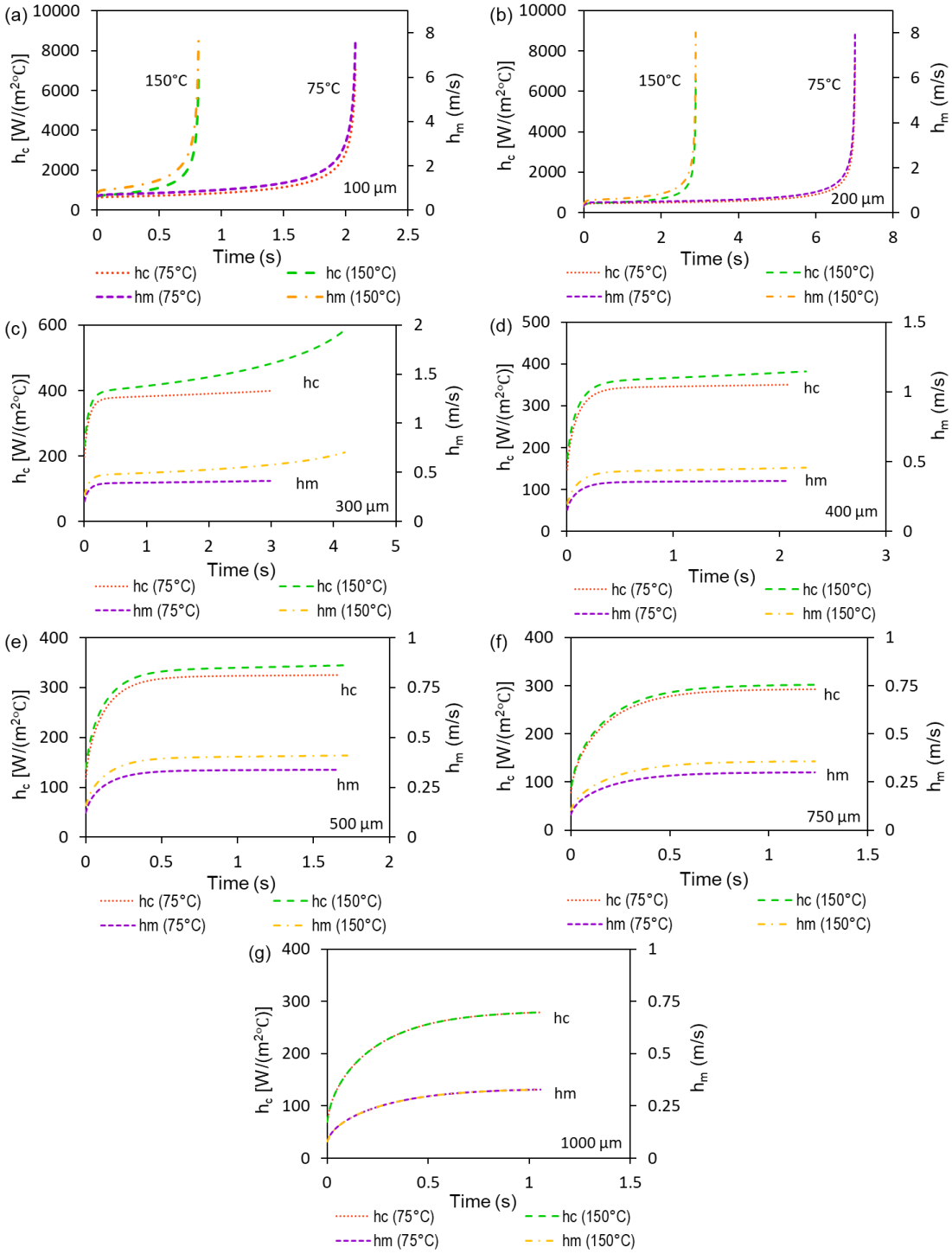

Figure 9. The heat and mass transfer coefficient of the droplets for condition 1 and 2; (**a**) 100 µm; (**b**) 200 µm; (**c**) 300 µm; (**d**) 400 µm; (**e**) 500 µm; (**f**) 750 µm; and (**g**) 1000 µm.

These phenomena are also reflected in Figure 10, where the percent mass loss rates of the water droplets are presented for conditions 1 and 2. The highest percent mass loss rate was for the smallest droplet (100 µm), and the lowest percent mass-loss rate was for the largest droplet (1000 µm). The figure shows that the droplet with initial diameters of 100 µm and 200 µm remain suspended for 2.16 and 7.42 s, respectively, for condition 1, and 0.85 and 2.98 s, respectively, for condition 2. At these times, they have disappeared because of their completely evaporation. The data presented in Figure 10 demonstrate that, for condition 1, the percentage mass loss of droplets initially with diameters of 300, 400, 500 and 750 µm are 36%, 18%, 11% and 4%, respectively, and these losses are 88%, 42%, 24% and 9%, respectively, for condition 2. As a result, the droplets can reach the floor of the enclosure. The evaporation of the 750 µm and 1000 µm diameter droplets results in a negligible decrease in their diameters because of their relatively small surface-to-volume ratios and reaching the floor in the shortest time.

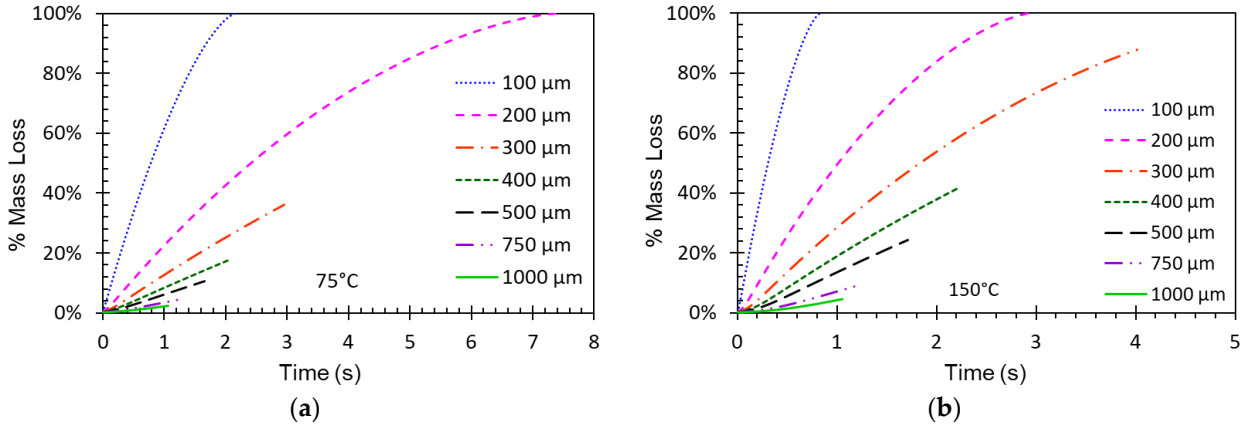

Figure 10. The mass loss of droplets with different initial diameters; (**a**) condition 1 (75 °C); (**b**) condition 2 (150 °C).

Water mists and water sprays both extract heat from the hot environment by convective heat transfer. The temperature of droplets is maintained lower resulting from the evaporation, which requires latent heat. The required heat for evaporation of individual droplets with the different initial diameters and one kilogram of droplets consisting of different initial sizes for conditions 1 and 2 is presented in Figure 11. The figure demonstrates that the amount of heat absorbed by a tiny individual droplet is much lower than that absorbed by an individual larger droplet in both cases. For example, in condition 1, a droplet with an initial diameter of 100 µm absorbs 1.35×10^{-3} J of heat, whereas a droplet with 1000 µm absorbs 40×10^{-3} J of heat. However, a given mass of water consists of droplets with 100 µm size containing 1000 times more droplets than the same amount of water consisting of droplets with 1000 µm size. As a result, 1 kg of droplets with 100 µm extracts about 2600 kJ of energy from its surrounding environment, whereas the same mass of water containing 1000 µm droplets extracts only about 76 kJ. This indicates one of the key attributes of fine sprays in suppressing fires: 1 kg of water consisting of 200 µm droplets also absorbs the same amount of energy as that of 100 µm droplets. This is due to the reason that both sizes of the droplets are evaporated entirely in the air.

The droplets in condition 2 absorbed a larger amount of heat compared to that of condition 1, due to the higher air temperature of condition 2. The difference of absorbed heat by the single droplets and 1 kg of droplets is not much (about 3%) for 100, and 200 µm droplets as both have evaporated in both conditions. However, this difference is significant (about 130%) for 300 µm and higher diameter because the equilibrium temperature at condition 2 is higher than that of condition 1. As a result, the droplets have absorbed a higher amount of heat. However, the heat absorbed by the individual droplets and 1 kg of water consisting of droplets has followed a similar trend.

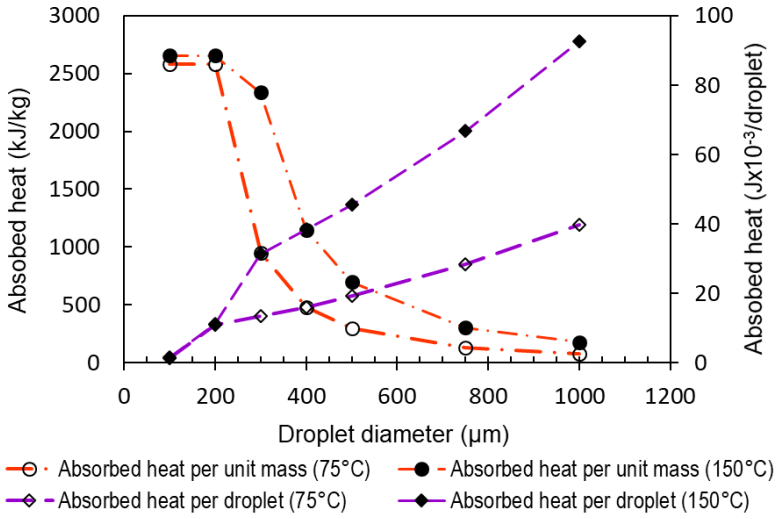

Figure 11. Absorbed heat by the droplets with different initial diameters for condition 1 and 2.

5. Conclusions

In this study, investigations have been performed on the behaviour of individual water-mist droplets travelling through a hot air layer induced by a room fire. A previously developed and validated quasi-physical model has been used to perform the work. The initial size of droplets has been varied, and the temperature profiles, locations, velocity trajectories, evaporation rates and the absorption of heat by the falling droplets have been predicted. The finding of the study can be summarised as below:

(a) The equilibrium thermal condition of droplets is independent of the initial size and temperature of droplets. Instead, it depends principally on the temperature and relative humidity of ambient air.

(b) The smaller size of droplets (in this study, 100 and 200 μm) can evaporate entirely before reaching the floor. This is because the low terminal velocity of droplets and rapid evaporation due to tiny in size have facilitated them to disappear completely before reaching the floor. On the other hand, the larger size of droplets (≥300 μm) has reached the floor within a shorter time and with a small amount of evaporation.

(c) Notably, smaller droplets are more effective in absorbing heat energy from the hot air per unit mass of water. This is because the smaller droplet has a significant amount of evaporation and takes a longer time to reach the floor or may evaporate entirely before reaching the floor.

(d) Therefore, in the case of fire extinguishment, the smaller size of droplets (in this case, 100 and 200 μm) may be effective in cooling the air within an enclosure; but they are less likely to penetrate a layer of hot air and extinguish conflagrating surfaces on the floor of an enclosure. On the other hand, droplets with a larger diameter are more effective in impingement of a smoke layer, but the larger droplet does not contribute significantly in absorbing heat from the surrounding.

The WDEM model has been shown to be useful for analysing the effects of initial diameters of droplets when they are exposed to fire-induced hot environments. Furthermore, the generality of the heat and mass transfer model enables it to be used to develop parametric models for a wide range of environments and droplet sizes. The results show that the smaller droplets of spray effectively cool the environment due to their rapid evaporation, and the larger droplets are effective in impinging the layer hot air or smoke in a fire environment. The findings of this study can be helpful in evaluating and designing the effective sizes of droplets or a group of droplets for a particular fire situation.

This study will be further extended to consider the effect of the interaction of droplets, injection velocity, distribution of droplet sizes, the effect of different initial velocity of air and droplets, and also the effect of humidification of air due to evaporation of droplets.

Author Contributions: H.M.I.M. developed the model. H.M.I.M., G.T. and K.A.M.M. contributed in conceptualisation, development of the background theory and formulations of the model. The text of the paper was formed by H.M.I.M.; K.A.M.M. and G.T. edited the paper and supervised the research direction. All authors have read and agreed to the published version of the manuscript.

Funding: The authors wish to acknowledge the technical and financial assistance provided by Defence Science and Technology Organisation (DSTO), Australia.

Institutional Review Board Statement: Not applicable.

Informed Consent Statement: Not applicable.

Data Availability Statement: Not applicable.

Conflicts of Interest: The authors declare no conflict of interest.

Nomenclature

A	surface area, m^2
Bi	biot number
C_d	drag coefficient
c_{pa}	specific heat capacity of air, J/(kg·°C)
c_{pw}	specific heat capacity of water, J/(kg·°C)
D	diameter, m
F	view factor
g	acceleration due to gravity, m/s^{-2}
h_c	convective heat transfer coefficient, $W/(m^2 \cdot °C)$
h_m	mass transfer coefficient, m/s
k	conductivity, J/m·°C
L	latent heat of vaporisation of water, J/kg
m	mass, kg
Nu	Nusselt number
p	vapour pressure, Pa
Pr	Prandtl number
P	pressure, Pa
R	universal gas constant, J/(K·mol)
Re	Reynolds number
RH	relative humidity, %
Sc	Schmidt number
Sh	Sherwood number
T	temperature, °C
t	time, s
V	volume, m^3
v	air-droplet relative velocity, m/s
y	vertical distance from the mist nozzle, m
z	height, m
Greek symbols	
α	thermal diffusivity, m^2/s
μ	dynamic viscosity, Pa·s
v	kinematic viscosity, m^2/s
ρ	density, kg/m^3
ε	emissivity factor
D	mass diffusivity coefficient
σ	Stefan–Boltzmann constant, $W/(m^2 \cdot K^4)$

Subscripts	
a	air
AB	binary system of A and B
bw	boundary wall
c	convective heat
d	drag
e	evaporation
f	flame
g	gravitation/gas
proj	projected area
s	droplet surface
w	water
∞	refers to the far-field value

References

1. Yang, P.; Liu, T.; Qin, X. Experimental and numerical study on water mist suppression system on room fire. *Build. Environ.* **2010**, *45*, 2309–2316. [CrossRef]
2. Kim, S.C.; Ryou, H.S. An experimental and numerical study on fire suppression using a water-mist in an enclosure. *Build. Environ.* **2003**, *38*, 1309–13016. [CrossRef]
3. *NFPA 750*; Standard on Water Mist Fire Protection Systems. National Fire Protection Association: Quincy, MA, USA, 2010.
4. Liu, J.; Liao, G.; Li, P.; Fan, W.; Lu, Q. Progress in research and application of water-mist fire suppression technology. *Chin. Sci. Bull.* **2003**, *48*, 718–725. [CrossRef]
5. Mahmud, H.M.I.; Moinuddin, K.A.M.; Thorpe, G.R. Experimental and numerical study of high-pressure water-mist nozzle sprays. *Fire Saf. J.* **2016**, *81*, 109–117. [CrossRef]
6. Beji, T.; Thielens, M.; Merci, B. Assessment of heating and evaporation modelling based on single suspended water droplet experiments. *Fire Saf. J.* **2019**, *106*, 124–135. [CrossRef]
7. Volkov, R.S.; Strizhak, P.A. Planer laser-induced fluorescence diagnostics of water droplets heating and evaporation at high-temperature. *Appl. Therm. Eng.* **2017**, *127*, 141–156. [CrossRef]
8. Strizhak, P.; Volkov, R.; Castanet, G.; Lemoine, F.; Rybdylova, O.; Sazhin, S. Heating and evaporation of suspended water droplets: Experimental studies and modelling. *Int. J. Heat Mass Tran.* **2018**, *127*, 92–106. [CrossRef]
9. Sobac, B.; Talbot, P.; Haut, B.; Rednikov, A.; Colinet, P. A comprehensive analysis of the evaporation of a liquid spherical drop. *J. Colloid Interface Sci.* **2015**, *438*, 306–317. [CrossRef]
10. Thielens, M.; Merci, B.; Beji, T. Development of a novel two-zone model for the heating of an evaporating liquid droplet. *Fire Saf. J.* **2021**, *120*, 103019. [CrossRef]
11. Mahmud, H.M.I.; Moinuddin, K.A.M.; Thorpe, G.R. Study of water-mist behaviour in hot air induced by a room fire: Model development, validation and verification. *Fire Mater.* **2016**, *40*, 190–205. [CrossRef]
12. Chow, W.K.; Yao, B. Numerical modeling for interaction of a water spray with smoke layer. *Numer. Heat Transf.* **2001**, *39*, 267–283. [CrossRef]
13. Cooper, L.Y. The interaction of an isolated sprinkler spray and a two-layer compartment fire environment. *Int. J. Heat Mass Transf.* **1995**, *38*, 679–690. [CrossRef]
14. Chow, W.K.; Tong, A.C. Experimental studies on sprinkler water spray-smoke layer interaction. *J. Appl. Fire Sci.* **1995**, *4*, 171–184. [CrossRef]
15. Chow, W.K.; Cheung, Y.L. Simulation of Sprinkler-Hot Layer Interaction Using a Field Model. *Fire Mater.* **1994**, *18*, 359–379. [CrossRef]
16. Morgan, H.P. Heat transfer from a buoyant smoke layer beneath a ceiling to a sprinkler spray. 1—A tentative theory. *Fire Mater.* **1979**, *3*, 27–33. [CrossRef]
17. Morgan, H.P.; Baines, K. Heat Transfer from a Buoyant Smoke Layer Beneath a Ceiling to a Sprinkler Spray. 2—An Experiment. *Fire Mater.* **1979**, *3*, 34–38. [CrossRef]
18. John, V.V. A full-scale experiment study of water mist spray convection. In Proceedings of the 2nd International Conference on Fire Research and Engineering, Gaithersburg, MD, USA, 3–8 August 1997; pp. 282–289.
19. Chow, W.K. On the evaporation effect of a sprinkler water spray. *Fire Technol.* **1989**, *25*, 364–373. [CrossRef]
20. Li, S.C.; Yang, D.; Huo, L.H.; Li, Y.Z.; Wang, H.B. Studies of cooling effects of sprinkler spray on smoke layer. In *Fire Safety Science, Proceedings of the Ninth International Symposium, International Association of Fire Safety Science*; University of Karlsruhe: Karlsruhe, Germany, 2008; pp. 861–872.
21. Floyd, J.; McDermott, R. Development and evaluation of two new droplet evaporation schemes for fire dynamics simulations. *Fire Saf. J.* **2017**, *91*, 643–652. [CrossRef]
22. Liu, Z.; Kim, A.K. A review of water mist fire suppression systems-fundamental studies. *J. Fire Prot. Eng.* **2000**, *10*, 32–50. [CrossRef]
23. Grant, G.J.; Brenton, J.; Drysdale, D. Fire suppression by water sprays. *Prog. Energy Combust. Sci.* **2000**, *26*, 79–130. [CrossRef]

24. Liu, Z.; Kim, A.K. A review of water mist fire suppression technology: Part II- Application studies. *J. Fire Prot. Eng.* **2001**, *11*, 16–42. [CrossRef]
25. Rashbash, D.J.; Rogowski, Z.W.; Stark, G.W.V. Mechanism of extinction of liquid fires with water sprays. *Combust. Flame* **1960**, *4*, 223–234. [CrossRef]
26. Shu, Y.L.; Jeng, W.J.; Chiu, C.W.; Chen, C.H. Assessment of fire protection performance of water mist applied in exhaust ducts for semiconductor fabrication process. *Fire Mater.* **2005**, *29*, 295–302. [CrossRef]
27. Yao, B.; Chow, W.K. Extinguishment of a PMMA fire by water spray with high droplet speeds. *Int. J. Therm. Sci.* **2005**, *44*, 410–419. [CrossRef]
28. Back, G.G.; Beyler, C.L.; DiNenno, P.J.; Hansen, R.; Zalosh, R. *Full-Scale Testing of Water Mist Fire Suppression Systems in Machinery Spaces*; CG-D-26-98; United States Coast Guard: Washington, DC, USA, 1998.
29. Mawhinney, J.R.; Dlugogorski, B.Z.; Kim, A.K. A closer look at the fire extinguishing properties of water mist. Fire Safety Science. In Proceedings of the 4th International Symposium on Fire Safety Science, Ottawa, ON, Canada, 13–17 July 1994; pp. 47–60.
30. Wighus, R. Engineering relations for water mist fire suppression systems. In Proceedings of the Halon Alternatives Technical Working Conference, Albuquerque, NM, USA, 30 April–1 May 1995; p. 397.
31. Novozhilov, V. Flashover control under fire suppression conditions. *Fire Saf. J.* **2001**, *36*, 641–660. [CrossRef]
32. Li, Y.F.; Chow, W.K. Study of water droplet behaviour in hot air layer in fire extinguishment. *Fire Technol.* **2008**, *44*, 351–381. [CrossRef]
33. Vaari, J. A transient one-zone computer model for total flooding water mist fire suppression in ventilated enclosures. *Fire Saf. J.* **2002**, *37*, 229–257. [CrossRef]
34. Barrow, H.; Pope, C.W. Droplet evaporation with reference to the effectiveness of water-mist cooling. *Appl. Energy* **2007**, *84*, 404–412. [CrossRef]
35. Katsios, X.K.; Krikkis, R.N. Effect of surface tension and evaporation on phase change of fuel droplets. *Heat Transf. Eng.* **2001**, *22*, 33–40. [CrossRef]
36. Holman, J.P. *Heat Transfer*, 9th ed.; McGraw-Hill Book Company: New York, NY, USA, 2002; p. 133.
37. Chelliah, H.K. Flame inhibition/suppression by water mist: Droplet size/surface area, flame structure, and flow residence time effects. *Proc. Combust. Inst.* **2007**, *31*, 2711–2719. [CrossRef]
38. Ananth, R.; Mowrey, R.C. Ultra-Fine Water Mist Extinction Dynamics of a Co-Flow Diffusion Flame. *Combust. Sci. Technol.* **2008**, *180*, 1659–1692. [CrossRef]
39. Hua, J.S.; Kumar, K.; Khoo, B.C.; Xue, H. A numerical study of the interaction of water spray with a fire plume. *Fire Saf. J.* **2002**, *37*, 631–657. [CrossRef]
40. Sikanen, T.; Vaari, J.; Hostikka, S.; Paajanen, A. Modeling and Simulation of High Pressure Water Mist Systems. *Fire Technol.* **2014**, *50*, 483–504. [CrossRef]
41. Bullen, M.L. The effect of a sprinkler on the stability of a smoke layer beneath a ceiling. *Fire Technol.* **1977**, *13*, 21–34. [CrossRef]
42. *ASHRAE Handbook: Fundamentals*; American Society of Heating, Refrigeration and Air Conditioning Engineers. Inc.: New York, NY, USA, 1985; p. 5.5.
43. William, C.H. *Aerosol Technology*; John Wiley & Sons Inc.: New York, NY, USA, 1999.
44. Bird, R.B.; Stewart, W.E.; Lightfoot, E.N. *Transport Phenomena*; John Willy and Sons, Inc.: New York, NY, USA, 1960; pp. 59, 505.
45. Beard, K.V.; Pruppacher, H.R. A wind tunnel investigation of the rate of evaporation of small water drops falling at terminal velocity in air. *J. Atmos. Sci.* **1971**, *28*, 1455–1464. [CrossRef]
46. Cengel, Y.A.; Turner, R.H. *Fundamental of Thermal Fluid Sciences*, 2nd ed.; McGraw-Hill Book Company: New York, NY, USA, 2005; pp. 1088–1089.
47. Smolik, J.; Dzumbova, L.; Schwarz, J.; Kulmala, M. Evaporation of ventilated water droplet: Connection between heat and mass transfer. *Aerosol Sci.* **2001**, *32*, 739–748. [CrossRef]
48. Brown, P.P.; Lawler, D.F. Sphere drag and settling velocity revisited. *J. Environ. Eng. (ASCE)* **2003**, *129*, 222–231. [CrossRef]
49. Gunn, R.; Kinzer, G.D. The terminal velocity of fall for water droplets in stagnant air. *J. Meteorol.* **1949**, *6*, 243–248. [CrossRef]
50. McGrattan, K.; McDermott, R.; Vanella, M.; Hostikka, S.; Floyd, J. *Fire Dynamics Simulator (Version 6), Technical Reference Guide, Volume 1: Mathematical Model*, 6th ed.; NIST Special Publication 1018-1, Revision: FDS6.7.4-0-gbfaa110; National Institute of Standards and Technology (NIST), U.S. Department of Commerce: Gaithersburg, MD, USA, 2021.
51. Vendel, J. Aerosols collection by spray water drops: Experimental results and model. In Proceedings of the Cooperative Severe Accident Research Program Meeting, Bethesda, MD, USA, May 1998.
52. Plumecocq, W.; Audouin, L.; Joret, J.P.; Pretrel, H. Numerical method for determining water droplets size distributions of spray nozzles using a two-zone model. *Nucl. Eng. Des.* **2017**, *324*, 67–77. [CrossRef]
53. *NFPA 13*; Automatic Sprinkler Systems Handbook. National Fire Protection Association: Quincy, MA, USA, 2007; p. 119.
54. Li, D.; Zhu, G.; Zhu, H.; Yu, Z.; Gao, Y.; Jiang, X. Flame spread and smoke temperature of full-scale fire test of car fire. *Case Stud. Therm. Eng.* **2017**, *10*, 315–324. [CrossRef]
55. Pretrel, H.; Varrall, K.; Vauquelin, O.; Audouin, L. Smoke induced flow in two rooms mechanically ventilated and linked with a horizontal vent type opening. In Proceedings of the 11th International Symposium of Fire Safety Science, University of Canterbury, Christchurch, New Zealand, 10–14 February 2014; pp. 486–498. [CrossRef]

56. Jeong, J.Y.; Ryou, H.S. A Study on Smoke Movement in Room Fires with Various Pool Fire Location. *KSME Int. J.* **2002**, *16*, 1485–1496. [CrossRef]
57. Zhou, J.; Mao, J.; Huang, Y.; Xing, Z. Studies on Smoke Temperature Distribution in a Building Corridor Based on Reduced-scale Experiments. *J. Asian Archit. Build. Eng.* **2017**, *16*, 341–348. [CrossRef]
58. Lefebvre, A.H.; McDonell, V.G. *Atomization and Sprays*; CRC Press: Boca Raton, FL, USA, 2017; p. 247. [CrossRef]
59. Zhou, Y.; Bu, R.; Zhang, X.; Fan, C.; Gong, J. Performance evaluation of water mist fire suppression: A clean and sustainable fire-fighting technique in mechanically-ventilated place. *J. Clean Prod.* **2019**, *209*, 1319–1331. [CrossRef]